Attenuated Total Internal Reflection Infrared Mapping Microspectroscopy of Soft Materials

LORI L. LEWIS and ANDRÉ J. SOMMER*

Molecular Microspectroscopy Laboratory, Department of Chemistry and Biochemistry, Miami University, Oxford, Ohio 45056

Attenuated total internal reflection (ATR) infrared mapping microspectroscopy of soft samples is reviewed and investigated by using cartridge-based germanium hemispheres. The study demonstrates the use of these devices for obtaining line scans or maps of soft pliable surfaces over an area of approximately 100 × 100 micrometers. An experimental determination of the spatial resolution by using a cross-sectioned polymer film showed a twofold improvement over transmission infrared microspectroscopy for sample sizes at the diffraction limit. Optical details of the devices are discussed in the context of ATR measurements in addition to their application for the study of polymer laminates often encountered in industry and forensics.

Index Headings: **ATR microspectroscopy; Infrared microspectroscopy; Surface analysis; Polymer laminates.**

INTRODUCTION

Attenuated total internal reflection (ATR) infrared microspectroscopy is becoming a well-established analytical tool due to the inherent advantages associated with its macro counterpart and several specific to the micro configuration.[1–8] In addition to the ability to analyze strongly absorbing samples with little preparation, the micro adaptation has the added benefits of higher and more reproducible contact pressures applied to the sample and the ability to analyze small particulates and/or spatial domains that can be part of a much larger sample.[2,4,8–10] In comparison to normal transmission infrared microspectroscopy, ATR infrared microspectroscopy can interrogate spatial domains that are two times smaller without the effects associated with diffraction.[8,9] While conventional point probe ATR microspectroscopy for the study of rigid surfaces has been demonstrated, the study of soft pliable surfaces such as polymer laminates or tissue sections has been somewhat more problematic.

Conventional ATR microspectroscopy can be conducted on soft surfaces; however, point-by-point mapping is experimentally difficult and severely limited with respect to time. In order to obtain the contact pressure necessary to record a spectrum, with the use of a point ATR probe, the sample surface must be deformed. Since the sample can be elastic, there is no guarantee it will have sufficient memory to relax and allow the adjacent points to be analyzed both reproducibly and systematically. In addition, the mobility of any surface residue on the sample may require that the probe tip be cleansed between each spatial sampling.

To overcome these problems, researchers have taken several approaches. Nakano and Kawata reported on the use of germanium hemispheres employed on a purpose-built evanescent field scanning microscope.[12,13] This particular instrument was confocal in that both the source and detector were apertured to provide better spatial isolation. As shown in Fig. 1 (adapted from their work), the sample is mounted to the bottom of the germanium hemisphere, and both hemisphere and sample are scanned beneath the infrared microscope with a piezo-electric controlled stage. Nakano and Kawata demonstrated the ability to achieve subwavelength resolution with an improvement factor of 4× relative to a normal reflection measurement. One limitation associated with this geometry is that the scan length for a given map is limited to approximately 100 μm. This limitation arises from increasing optical aberrations, such as astigmatism, as the hemisphere is translated off-axis. However, the advantages of this approach include a high numerical aperture and a magnification factor equal to the refractive index of the crystal. The magnification factor arises from the hemispherical geometry and the refractive index of the crystal. This factor allows one to work with remote apertures that are four times larger for a given sample, thereby circumventing problems associated with diffraction, while still maintaining a relatively high signal throughput.[8] Esaki et al. have employed specially fabricated KRS-5 chevrons and an infrared microscope to obtain maps of soft surfaces.[11] Figure 1, adapted from their work, shows this geometry with the sample clamped to the inside surface of the chevron. A spatial resolution on the order of 25 μm was obtained over several millimeters in length. This approach has the benefit of being able to obtain line scans over greater lengths without off-axis aberrations, but because of its geometry, has the disadvantages of possessing no magnification factor and a limited numerical aperture. A ray trace of light entering the chevron from a conventional infrared objective (numerical aperture of 0.60) shows that the chevron limits the numerical aper-

Received 19 January 1999; accepted 4 October 1999.

* Author to whom correspondence should be sent.

0003-7028/00/5402-0324$2.00/0

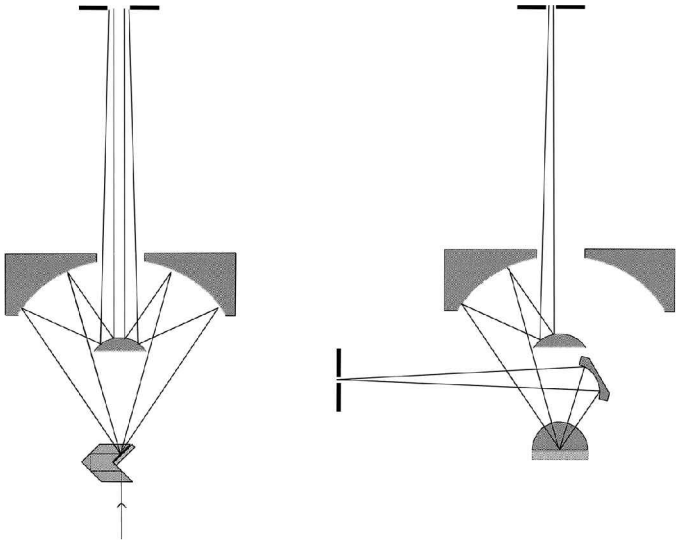

FIG. 1. Optical configurations for ATR mapping microspectroscopy after Esaki et al. (left) and Nakano and Kawata (right).

ture to a value of approximately 0.1. In comparison, the germanium hemisphere enhances the numerical aperture of the objective to a value of 2.4. The reduced numerical aperture and nonexistent magnification factor severely limit the spatial resolution and the light throughput of the chevron. Another disadvantage of the chevron design is that the rays impinge upon the crystal face at an average angle of 26°. Although front surface reflection losses are lower for the chevron (~ 17% compared to ~ 36% for the hemisphere) there will be a 5% difference in the transmission of *s*- and *p*-polarized light through the crystal. For the hemisphere, the rays enter the crystal near normal and thus exhibit minimal polarization effects. Taken as a whole, the benefits of the hemisphere far outweigh those of the chevron when spatial resolution and throughput are considered. As such, we have undertaken a study using an approach similar to that of Nakano and Kawata, but using a conventional infrared mapping microscope and cartridge-based germanium hemispheres. We have previously reported on the use of these devices for the study of isolated particulates and the experimental considerations for their use.[8] Major differences between the instrument employed in this study and that of Nakano and Kawata include the use of a single aperture after the sample and global illumination of the sample. This configuration circumvents the need to move the source aperture with the hemisphere, but at the anticipated expense of spatial resolution. Pertinent questions to be addressed include the spatial resolution of the approach and its implementation on a standard infrared microscope.

EXPERIMENTAL

A Perkin-Elmer Spectrum 2000 FT-IR spectrometer coupled with an *i*-Series microscope was employed in this investigation. The system utilized a 250 × 250 μm liquid nitrogen-cooled medium-band HgCdTe detector and a 215 × 100 mm x-y motorized mapping stage with incremental steps of one micrometer. The microscope stage and data collection were controlled with Perkin-Elmer's IMAGE (infrared microspectroscopy automated graphical environment) software. Axial adjustments were made at each sampling point to eliminate the loss in resolution from astigmatic aberrations noted by Nakano.[12]

The germanium cartridges employed in the investigation were obtained from Harrick Scientific Corporation (Catalog #USS-ATRJ). Details on their use and modification for infrared microspectoscopy have been described in a previous publication.[8]

All spectra reported in this investigation are the result of signal averaging 512 scans at 4 cm^{-1} resolution, unless otherwise noted. The approximate time to accumulate 512 scans was 7 min. Single-beam line scans were obtained by moving the microscope stage in 5 μm increments by using an aperture size corresponding to a 6 μm sample size. All positional displacements referred to are those at the sample, unless noted otherwise.

A cross-sectioned piece of photographic film with a thickness of 10 μm was employed to determine the spatial resolution of the method. The film was mounted onto the crystal face of the hemisphere with the use of a backing plate as described previously.[8] It consisted of a large substrate made of polyvinyl acetate (PVAc) and dye layers made of gelatin.

RESULTS AND DISCUSSION

Initial experiments conducted in the investigation dealt with the alignment of the hemisphere in the microscope. Since the germanium hemisphere is not visibly transparent, a means had to be developed to establish its center at the focus of the infrared beam. This task was accomplished by preliminary manual adjustment using the energy meter followed by the collection of a two-dimensional map of the hemisphere's face over an area of 600 × 600 μm (stage displacement). The map of the total absorbance for single-beam spectra exhibited low absorbances (i.e., high energy throughput) in the center, which decreased radially outward. The coordinates corresponding to the center of this map were then taken as the origin of the hemisphere. In a procedure to make alignment easier for subsequent scans, an index mark was scribed into the metal portion of the cartridge. With this index, one could easily find the center and focus of the hemisphere by moving the stage the appropriate offset distances.

Subsequent experiments were conducted to determine how precise the positioning of the hemisphere between background and sample scans needed to be. With the use of a single hemisphere, a background was recorded. The hemisphere was removed from the microscope, a sample was mounted, and the entire assembly was returned for the collection of a sample scan. Figure 2 illustrates spectra of an adhesive tape applied to the hemisphere taken by translating the hemisphere from the origin out to 10 μm. The background for these spectra was obtained with the hemisphere positioned at the origin. The spectra in the figure show rounded baselines, which are readily apparent for displacements as small as 3 μm from the origin. This distortion is the result of rays impinging the crystal off-normal causing a so-called off-axis aberration.[13] These data show that positioning of the hemisphere between background and sample scans needs to be better than 3 μm and that background spectra must be obtained at precisely the same off-axis position as are the

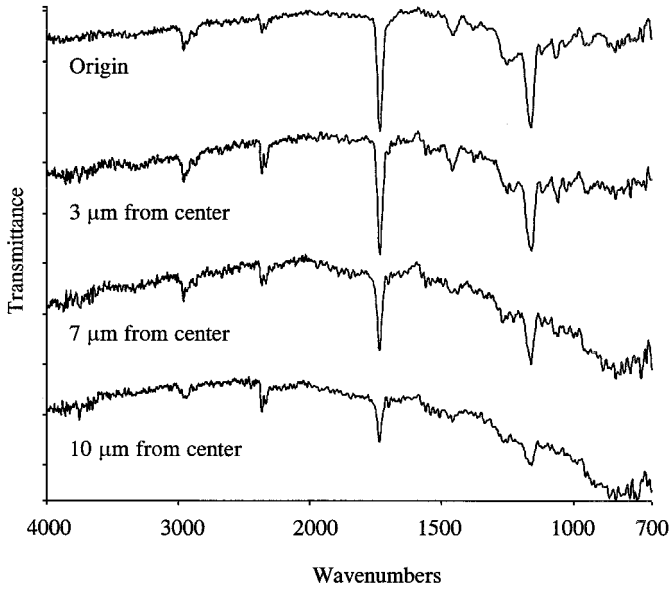

FIG. 2. Infrared spectra of an adhesive obtained with the hemisphere at various off-axis positions. Background obtained at origin of hemisphere.

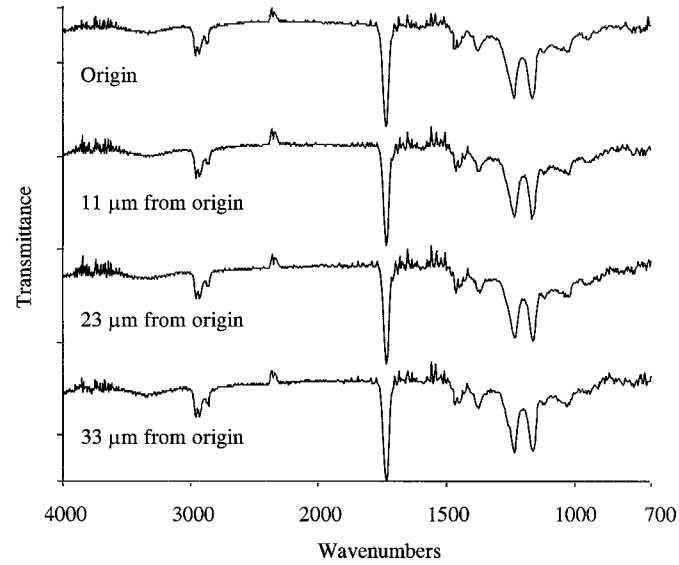

FIG. 3. Infrared spectra of an adhesive obtained with the hemisphere at various off-axis positions. Background obtained at identical off-axis positions as that of the sample spectra.

sample spectra. Figure 3 illustrates spectra of a similar adhesive, which have been obtained at off-axis positions as far out as 33 μm from the origin. Background spectra were collected at the same off-axis positions as the sample spectra. The spectra show no effects due to off-axis aberrations as shown by the flat baselines. More importantly, the signal-to-noise ratio (SNR) in each spectrum is constant, indicating that the light is not vignetted upon going to greater off-axis locations. Subsequent experiments demonstrated that the off-axis limit was approximately 50 μm, yielding a total range of 100 μm for the scan length.

One problem illustrated with the spectra in Fig. 3 is that of atmospheric compensation. Due to the lengthy time required to load a sample and the long scan times needed to generate a map, it was anticipated that atmospheric compensation would be a problem. As such, the feasibility of using an identical sister hemisphere to accumulate background scans was established. With the use of two hemispheres, one for the background and one for the sample, the time between the collection of the respective spectra could be reduced significantly, and background spectra could be collected at any time during a map. Figure 4 shows a comparison of spectra taken from a sample of adhesive tape, one with the background taken on the same hemisphere as the sample, the other with the background taken on the sister hemisphere. The spectra are qualitatively the same, and the signal-to-noise ratio is unaffected. The spectrum taken with the sister hemisphere for the background measurement clearly demonstrates better atmospheric compensation. Although there is a slightly sloping baseline, this effect was later taken care of by carefully selecting matched crystals. Matching the crystals was accomplished by measuring the light throughput for each crystal when positioned on-axis. Crystals with greater than 5% difference in energy throughput were not used.

Preliminary line scans of a structured sample, to determine the spatial resolution of the method, yielded results that did not correspond to the visible image of the mounted sample. Therefore, an optical ray trace of the light path entering the hemisphere was conducted (see Fig. 5). When the crystal is centered, incoming light is normal to the surface at all angles; thus the rays converge to the center of the hemisphere. As the hemisphere is displaced beneath the infrared beam in the positive or negative x-direction, the angle of refraction increases in both cases. This increase has the effect of displacing the beam in the positive and negative directions, respectively, thereby allowing a map to be generated. The change in the angle of light in the hemisphere, with respect to the hemisphere/sample interface, will also affect the penetration depth of the beam into the sample. For positive displacements the penetration depth decreases while it in-

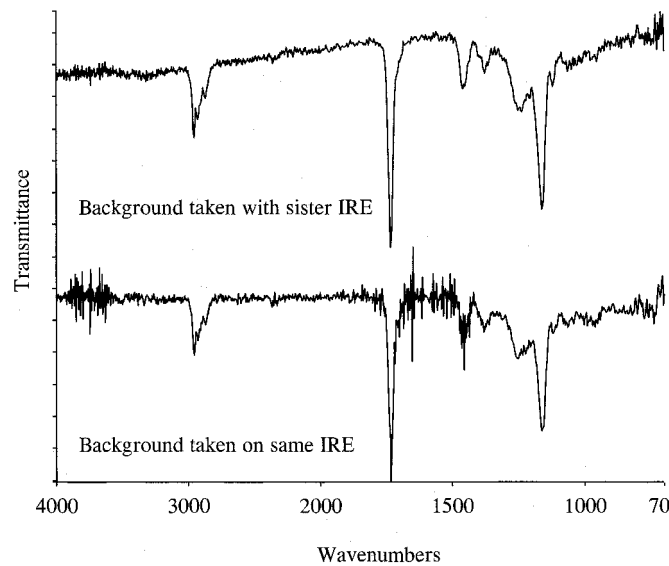

FIG. 4. Spectra collected on an adhesive with background obtained on same hemisphere (bottom) and sister hemisphere (top).

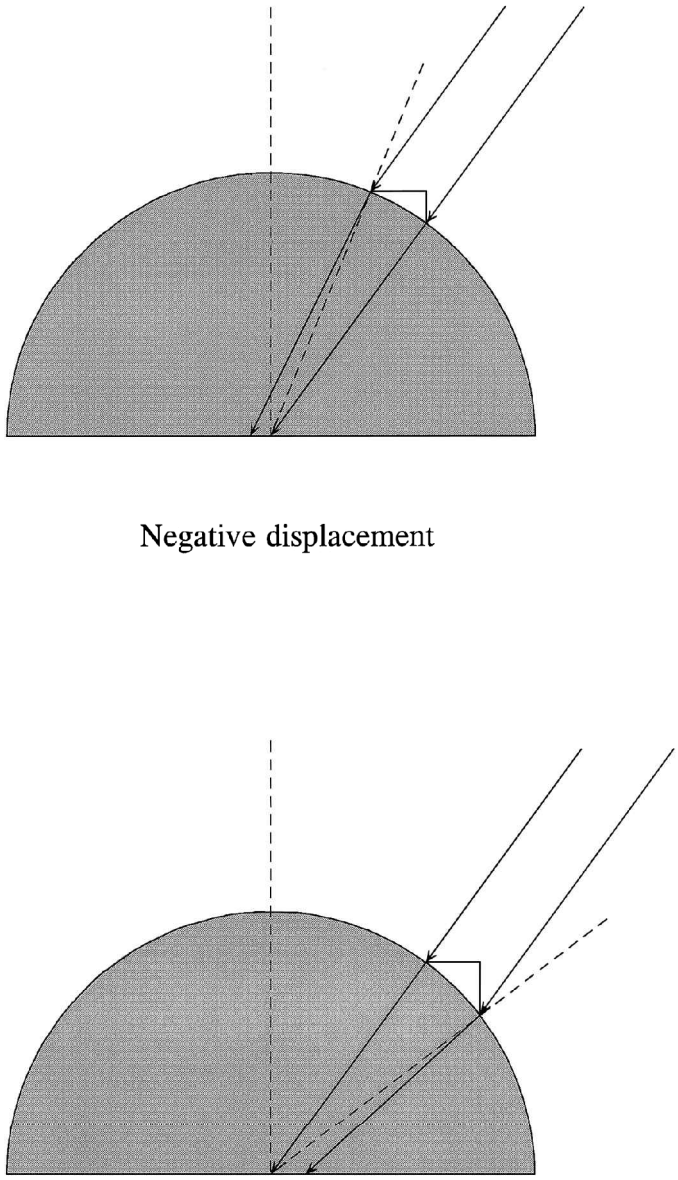

FIG. 5. Optical ray path of light traveling through the hemisphere for both negative and positive displacements.

creases for negative displacements. Table I summarizes characteristics that are important from the perspective of an ATR analysis. The data show that the light beam displacement within the hemisphere is approximately one third that of the stage displacement with the use of the current configuration. More important is the fact that the scan length in the negative x direction will be limited by the critical angle, which is, in turn, limited by the sample's refractive index. For an average angle of 26.5° and a sample refractive index of 1.5, the critical angle is 22°. This value corresponds to a beam displacement within the hemisphere of −41 μm. Finally, for any map the absorbances in each spectrum must be normalized against the penetration depth in order for the map to correspond with the visible image.

Taking these considerations into account, a line-scan of a structured sample was again attempted to determine the spatial resolution of the method. Figure 6 shows a thin cross section of a photographic film mounted in the sample hemisphere, and Fig. 7 exhibits infrared spectra extracted from a line map of the sample. The spectrum obtained at 12 μm above the origin of the hemisphere represents relatively pure gelatin, and at 12 μm below the center, the spectrum shows pure PVAc. Hence, this 24 μm distance gives an indication of the spatial resolution of the system. A more quantitative value was determined by obtaining the peak heights of the PVAc carbonyl band at 1746 cm^{-1} and the gelatin amide I band at 1651 cm^{-1} for all of the spectra in the line scan. These values were plotted against the beam displacement in the hemisphere in order to determine the spatial resolution (Fig. 8). Peak heights were normalized against the calculated penetration depths. With the use of a method similar to that of Gardiner et al. (i.e., generating a step function using the interface of the PVAc and gelatin layers and taking the ordinate distance corresponding to 5% and 95% of the maximum peak height), the spatial resolution determined from this plot is 22 μm.[14] A comparison of this value to the theoretical value of 6.1 μm shows that the experimental value is greater by a factor of 3.6×.

A detailed study of diffraction effects in infrared microscopes by Sommer and Katon[15] has shown that employing two apertures, one to target the source on the sample and one to target the illuminated sample onto the detector, reduces the effects of diffraction (stray light) compared to the use of a single aperture. This so-called dual masking or redundant aperturing reduces light illuminating areas outside the sample of interest until the size of the sample approaches the wavelength of the light. Beyond this ''diffraction limit'', closing the apertures further (over aperturing) will increase the amount of light falling in regions outside the sample.

Sommer and Katon have shown that, for an aperture setting corresponding to a sample size of 8 μm, the diameter of the sample actually viewed is some 6× larger.[15] For the ATR measurements with an aperture corresponding to a sample size of 6 μm, the area measured is some 3.6× larger. This improvement in spatial resolution for the ATR measurement may seem marginal, but it is significant when compared to a transmission measurement conducted on samples in this size domain. The results presented for the transmission measurements were for a confocal arrangement (i.e., apertures placed at both source and sample image), whereas the ATR measurements were conducted with one aperture placed at the sample image. This fact is also the reason the theoretical values observed by Nakano and Kawata were not observed in this investigation.[12] They employed a purpose-built confocal infrared microscope in their studies, which required tracking of both the source and sample apertures. In addition, the aperture setting for the ATR measurements is 25% smaller compared to those used for the transmission measurements. As such, one would expect a larger portion of the light falling outside the sample area. But as a result of the magnification factor of the hemisphere the aperture is larger, and as such, any oversampled area caused by diffraction is reduced.[8] This magnification factor and subsequent larger aperture size also

TABLE I. ATR characteristics as a function of stage displacement.[a]

Stage displacement	Angle in hemisphere	Beam displacement	Penetration depth	Stage displacement	Angle in hemisphere	Beam displacement	Penetration depth
0.00	26.50	0.00	1.00	0	26.50	0.00	1.00
−5.00	26.34	−1.56	1.02	5	26.77	1.56	0.97
−10.00	26.18	−3.11	1.04	10	27.03	3.14	0.94
−15.00	26.02	−4.65	1.07	15	27.30	4.72	0.92
−20.00	25.86	−6.19	1.09	20	27.57	6.30	0.89
−25.00	25.70	−7.72	1.11	25	27.84	7.90	0.87
−30.00	25.54	−9.24	1.14	30	28.11	9.50	0.85
−35.00	25.39	−10.75	1.17	35	28.38	11.11	0.83
−40.00	25.23	−12.26	1.20	40	28.65	12.73	0.81
−45.00	25.07	−13.76	1.23	45	28.92	14.35	0.79
−50.00	24.91	−15.26	1.26	50	29.19	15.99	0.78
−55.00	24.76	−16.75	1.30	55	29.47	17.63	0.76
−60.00	24.60	−18.23	1.34	60	29.74	19.28	0.75
−65.00	24.44	−19.71	1.39	65	30.01	20.94	0.73
−70.00	24.29	−21.18	1.44	70	30.29	22.61	0.72
−75.00	24.13	−22.65	1.49	75	30.56	24.28	0.71
−80.00	23.97	−24.10	1.55	80	30.84	25.97	0.69
−85.00	23.82	−25.56	1.62	85	31.11	27.66	0.68
−90.00	23.66	−27.00	1.70	90	31.39	29.37	0.67
−95.00	23.51	−28.45	1.79	95	31.66	31.08	0.66
−100.00	23.35	−29.88	1.89	100	31.94	32.80	0.65
−105.00	23.20	−31.31	2.01	105	32.22	34.54	0.64
−110.00	23.04	−32.74	2.16	110	32.50	36.28	0.63
−115.00	22.89	−34.16	2.35	115	32.78	38.03	0.62
−120.00	22.73	−35.57	2.60	120	33.06	39.79	0.61
−125.00	22.58	−36.98	2.94	125	33.34	41.56	0.60
−130.00	22.43	−38.38	3.46	130	33.62	43.34	0.60
−135.00	22.27	−39.78	4.41	135	33.90	45.14	0.59
−140.00	22.12	−41.17	7.13	140	34.19	46.94	0.58
−145.00	21.97	−42.56	∞	145	34.47	48.75	0.57

[a] All distance units are given in micrometers.

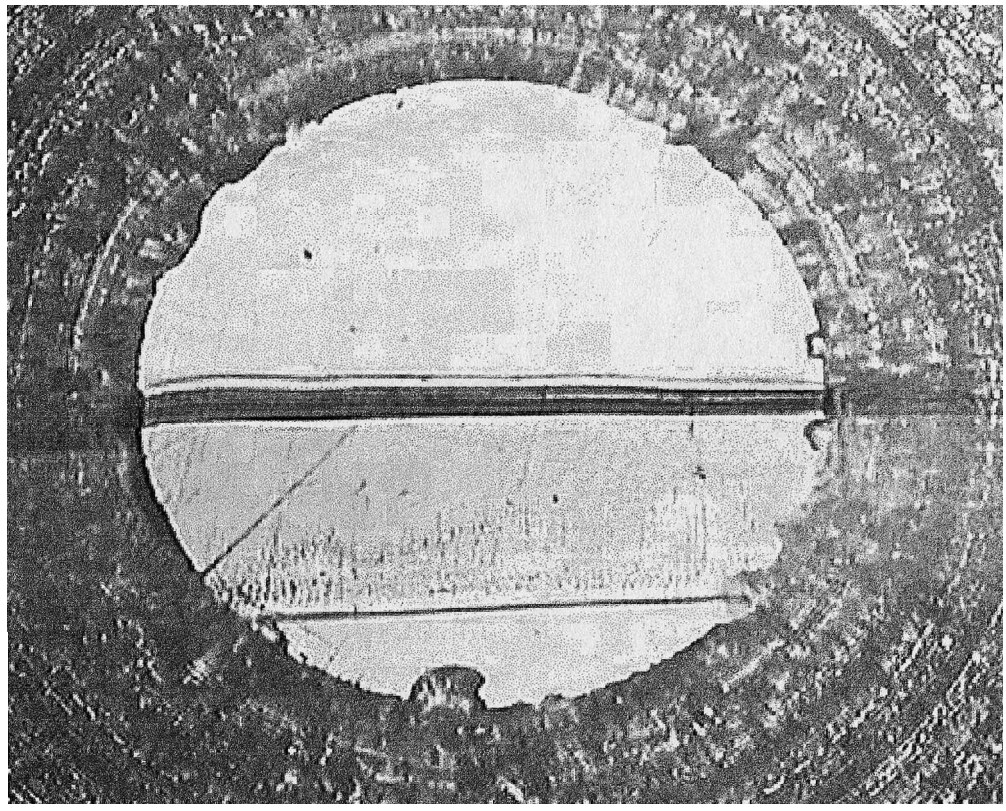

FIG. 6. Photomicrograph of photographic film mounted on the hemisphere.

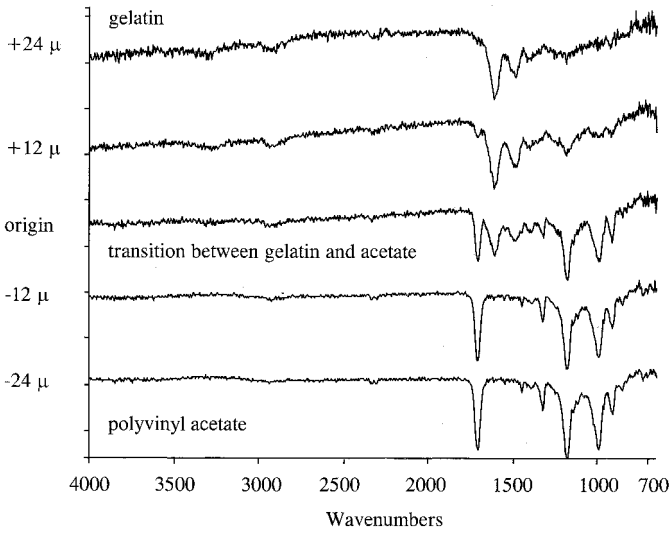

FIG. 7. Selected spectra obtained from a line scan of a cross-sectioned photographic film.

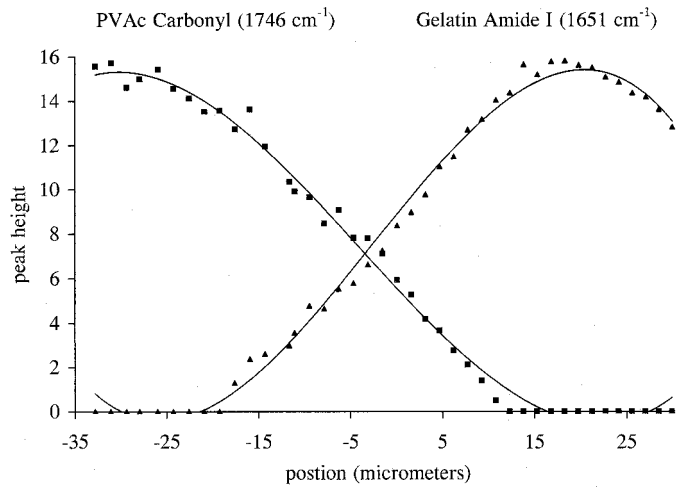

FIG. 8. Plot of peak height for the PVAc carbonyl (1746 cm^{-1}) and gelatin amide I (1651 cm^{-1}) as a function of displacement from the origin of the hemisphere.

increase the throughput of the measurement. Attempts to conduct the similar experiment in normal reflection geometry failed due to the fact that the aperture size corresponding to a 6 × 6 μm sample was not sufficient to allow a usable signal to be passed through the instrument.

The benefits to be gained by using this method include not only increased spatial resolution and throughput, allowing smaller samples to be analyzed, but the ability to analyze samples that have been traditionally difficult with the use of transmission infrared microanalysis. Figure 9 illustrates infrared spectra extracted from maps obtained on a commercial multi-layer laminate. At issue was the identification of 9 μm thick tie layer between polypropylene and polyvinylidene fluoride. The lower spectrum was recorded in transmission with an aperture corresponding to a sample size of 6 × 12 μm. The enlarged aperture was required to get sufficient energy through the system. The upper spectrum was recorded on the same sample by using identical scan parameters (e.g., coadditions, gain, etc.) but with the ATR configuration and an aperture corresponding to a sample size of 6 × 6 μm. The ATR spectrum can clearly be identified as ethylene/vinyl acetate.

A comparison of the spectra shows several advantages of using the ATR approach over that of transmission. First, the signal-to-noise ratio in the ATR spectrum is significantly higher than that of the transmission spectrum and remains constant over the entire spectrum. The SNR in the transmission spectrum decreases on going to longer wavelengths owing to diffraction.[8] From the standpoint of photometric accuracy, the absorbance of the C–H stretch and that in the region adjacent to this feature indicate that the sample is too thick and highly scattering. In preparation of the sample, however, the thickness employed was one in which the sample integrity could be guaranteed. Attempts to cut thinner cross sections failed due to the fact that the individual layers would delaminate from one another. In contrast, these problems and their associated spectral artifacts are absent from the ATR spectrum. Finally, a close comparison of the transmission spectrum shows that the absorptions located at 2838, 1453, and 1378 cm^{-1} are enhanced in the transmission spectrum relative to the carbonyl absorption located at 1737 cm^{-1}. These absorptions arise from polypropylene, indicating spectral contamination from the neighboring layer and reduced spatial resolution for the transmission measurement. Further evidence for this assignment comes from a consideration of the penetration depth as a function of wavelength in the ATR measurement. Due to the increased penetration depth for the absorptions located at 1453 and 1378 cm^{-1} relative to the carbonyl, one would expect these absorptions to be decreased in the transmission spectrum when in fact the trend is reversed.

CONCLUSION

We have demonstrated that ATR maps of small surfaces can be collected by using cartridge-based germanium hemispheres. The use of the devices on a conventional microscope allows one to improve the spatial resolution for sample sizes, at the diffraction limit, by a

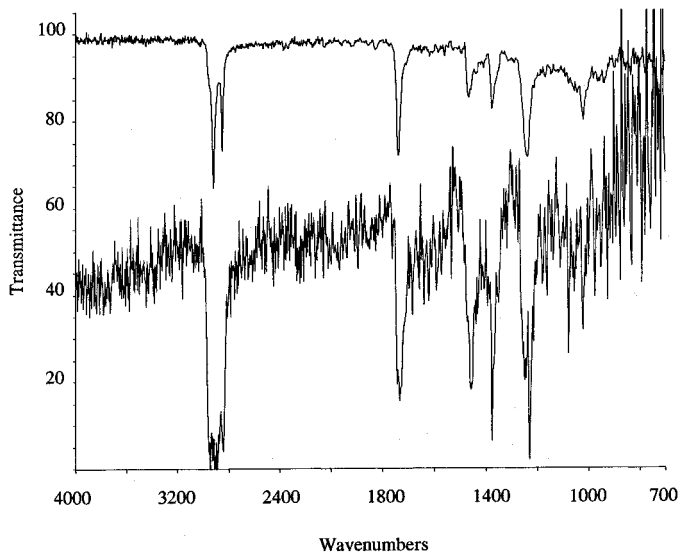

FIG. 9. Infrared spectra of a 9 μm thick ethylene/vinyl acetate tie layer obtained in transmission mode (bottom) and ATR mode (top).

factor of 2, compared to normal transmission measurements. The magnification factor associated with the hemisphere permits smaller samples to be interrogated with a reduction in the effects of diffraction. Care must be taken, however, in the interpretation of the results since the penetration depth varies when the hemisphere is scanned to different off-axis positions. A scan length of 100 μm is achievable, but this length is limited by the sample's refractive index and/or the hemisphere's refractive index.

We expect that the method will be most useful for those samples that require extremely thin cross sections for transmission analysis. These types of samples include multi-layer laminates made up of highly absorbing polymers and/or polymers that have been opacified with organic and inorganic fillers. Laminates that fall into this category include packaging materials and automotive finishes (forensics investigations). In both cases, and more so for the latter, significant sample preparation is required with the use of a microtome or a diamond anvil cell to achieve a suitable sample thickness.[16] Often this thickness is a compromise between the sample's optical and physical properties and the laboratory's budget. In contrast, the ATR method described in this report provides a suitable alternative that overcomes many of the drawbacks of transmission analysis for these types of samples. Future investigations will employ the two-dimensional aspects of the method that make it attractive for tissue samples.

ACKNOWLEDGEMENTS

The authors would like gratefully to acknowledge the support of the Perkin-Elmer Corporation, Procter and Gamble, and the Miami University Research Challenge Program.

1. J. A. Reffner, W. T. Wihlborg, and S. W. Strand, Am. Lab. **April,** 46 (1991).
2. N. J. Harrick, M. Milosevic, and S. L. Berets, Appl. Spectrosc. **45,** 944 (1991).
3. J. E. Katon and A. J. Sommer, Anal. Chem. **64,** 931A (1992).
4. J. A. Reffner, C. C. Alexay, and R. W. Hornlein, Proc. SPIE–Int. Soc. Opt. Eng. **1575** (8th International Conference on Fourier Transform Spectroscopy) 301 (1992).
5. P. A. Martoglio, in *Proceedings of the 28th Annual Meeting of the Microbeam Society,* J. J. Friel, Ed. (VCH Publishers, New York, 1994), pp. 95–96.
6. B. Yan, J. Fell, and G. Kumaravel, J. Org. Chem. **61,** 7467 (1996).
7. T. Tajima, S. Takeuchi, Y. Susuki, T. Tsuchibuchi, and K. Wada, Shimadzu Hyoron **53,** 55 (1996).
8. L. Lewis and A. J. Sommer, Appl. Spectrosc. **53,** 375 (1999).
9. J. A. Reffner and P. A. Martogio, Paper No. 551 presented at the 1994 Pittsburgh Conference on Analytical Chemistry and Spectroscopy, Chicago, Illinois (1994).
10. J. A. Reffner and P. A. Martoglio, ''Uniting Microscopy and Spectroscopy'', in *Practical Guide to Infrared Microspectroscopy,* Howard J. Humecki, Ed. (Marcel Dekker, New York, 1995), Chap. 2, p. 41.
11. Y. Esaki, K. Nakai, and T. Araga, Toyota Chuo Kenkyusho R & D Rebyu **30,** 57 (1995).
12. T. Nakano and S. Kawata, Bunko Kenkyu **41,** 377 (1992).
13. T. Nakano and S. Kawata, Scanning **16,** 368 (1994).
14. D. J. Gardiner, M. Bowden, and P. R. Graves, Philos. Trans. R. Soc. London, Ser., A **320,** 295 (1986).
15. A. J. Sommer and J. E. Katon, Appl. Spectrosc. **45,** 527 (1991).
16. S. G. Ryland, ''Infrared Microspectroscopy of Paint Evidence'', in *Practical Guide to Infrared Microspectroscopy,* Howard J. Humecki, Ed. (Marcel Dekker, New York, 1995), Chap. 6, pp. 177–180.